IOP Conf. Series: Materials Science and Engineering **231** (2017) 012031 doi:10.1088/1757-899X/231/1/012031

Wheel-rail profile matching based on finite element method for Beijing metro

LIU Jia-huan[1,a], ZHANG Jun[1]*, LIU Xiao-dong[1], ZHU Huang-shi[1], ZHANG Lin[2], ShangWeipeng[1]

[1] School of Mechatronics and Vehicle Engineering, Beijing University of Architecture and Technology, Beijing 102616, China;
[2] School of Traffic and Transportation Engineering, Dalian Jiaotong University, Dalian, Liaoning 116028, China

[a] Email:1015501612@qq.com, *Corresponding Authors: 58488408@qq.com.

Abstract. An instrument that measures wheel-rail appearance is used to measure the size of the wheel and rail in the section of the Baishiqiao South Station of Beijing Metro Line 6 to develop a finite element entity. Different working conditions such as axle load and traction are considered. The results show that: Under axle load, the matching performance of wheel I/rail II is improved, its contact area is the largest, and its equivalent stress and contact force are minimal; Under traction force, the matching performance of wheel I/rail II is improved, and the shear stress and equivalent stress are minimal, and thus is ideal.

1 Introduction

Beijing Metro Line 6 is a city rail line in the east-west direction. Experts worldwide have conducted extensive research on issues with regard to the matching of the wheel and rail surface1[1]. Meanwhile, Shevtsov [2-3] treated the rolling radius difference curve.

The typical wear wheel profile is selected, and the finite element software ABAQUS is used to create the wheel-rail geometric finite element contact model [4]. The mechanical properties of the wheel-rail profile under axle load and traction are compared, and the contact spot, contact force, and contact stress are compared [5].

2 Surface test method

In the subway vehicle operation process, wheel and rail wear is inevitable, as shown in Figure 1, for wheel and rail operation after a period of wear. A light band appears on the rail contact surface, and an uneven phenomenon occurs because of creep wheel wear [6].

(a) wheel wear situation

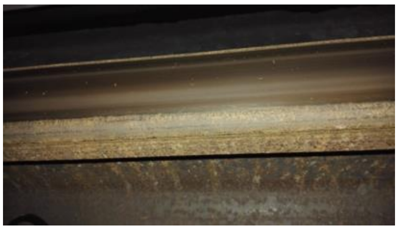

(b) wheel wear situation

Fig. 1 Wear of wheel and rail

Figure 2 is selected on the line of four different wear periods of the wheel wear surface comparison chart. The wheel tread wear is severe, and the rim is thin. In the middle of the tread, less wear is observed, and the flange part indicates increased wear. The tread on the outer side shows little wear. Finally, a flash is produced, implying plastic flow. In Figure 3, in the profile I surface for the standard 60-profile rail surface and the profile II surface for the selected wear-resistant rail surface, and a tip was observed on the inside of the rail, thereby resulting in plastic flow during rail wear [7].

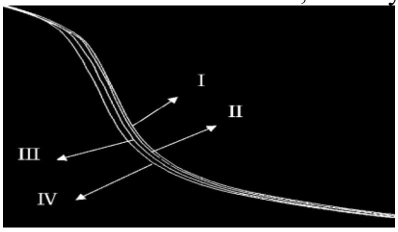

Fig. 2 Comparison of wheel profile

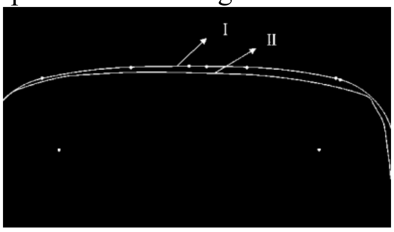

Fig. 3 Comparison of rail profile

3 Model established

The finite element software ABAQUS was used to establish the finite element model of the two-wheeled wheel and rail. Given that the spoke structure does not affect the wheel and the changes and distribution of rail contact force, the spokes were simplified, as shown in Figure 4.

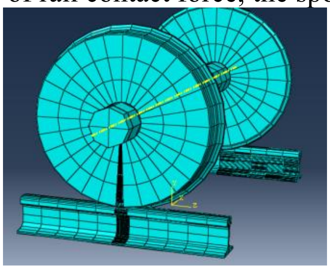

Fig. 4 Finite element model

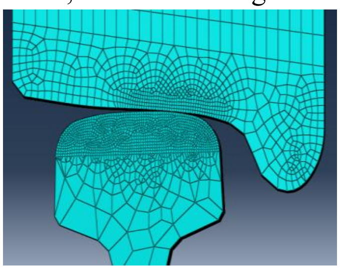

Fig. 5 Meshing of contact area

4. Calculation of results and analysis

4.1 Comparison of wear wheel/wear track and wear wheel/standard wheel

Figure 6 shows the comparison between the equivalent stress and contact pressure. The equivalent stress size is compared under the 1029 MPa wear wheel/standard rail matching condition. In addition, 829 MPa under the wear wheel/wear track condition is 19.9% lower than the former. This is the normal contact pressure comparison situation. Wheel/standard rail matching conditions for the 1993 MPa, wear wheel/wear rail matching conditions for 1045 MPa is 47.6% lower than the former.

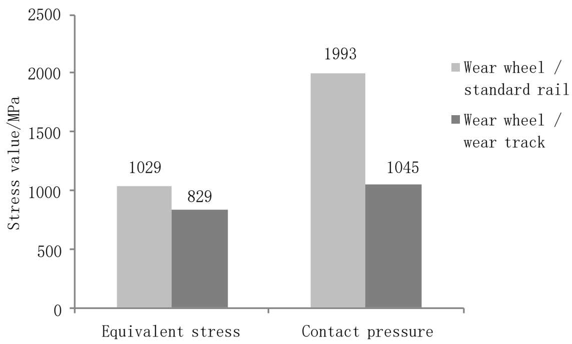

Fig. 6 Comparison of each index

4.2 Comparison of different wear wheels and the same wear track

The matching of wheel profiles I–IV with rail profile II is carried out to explore the matching mechanical properties of the wheel and rail profile under the two conditions. Figure 7 shows the distribution of contact spots of surface, and Table 1 shows the size of the contact area.

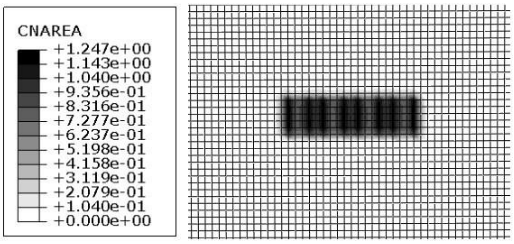

(a) Profile I wheels match profile II rails

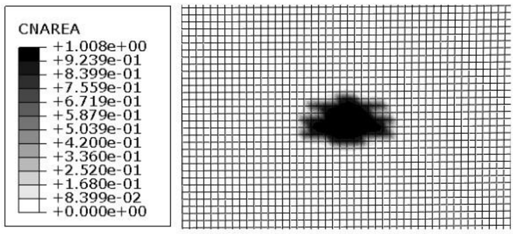

(b) Profile II wheels match profile II rails

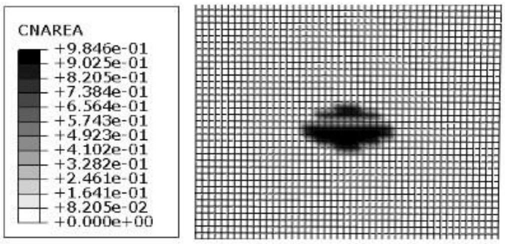

(c) Profile III wheels match profile II rails

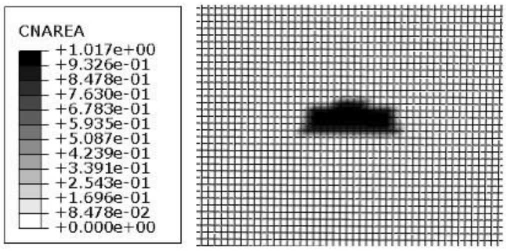

(d) Profile IV wheels match profile II rails

Fig. 7 Distribution of contact spots of surface

Table 1 Comparison of the size of contact area

Wheel / rail match	Contact spot area（mm^2）
Profile I wheels match profile II rails	119.186
Profile II wheels match profile II rails	63.4775
Profile III wheels match profile II rails	55.1467
Profile IV wheels match profile II rails	58.6002

As can be seen from Table 1, the contact spot area of the wheel profile I/rail profile II is the largest at 119.186 mm^2. Furthermore, the wheel profile I /rail profile II's contact areas are smaller than that in wheel profile II/rail profile II, wheel profile III/rail profile II, and wheel profile IV/rail profile II.

Figure 8 shows the equivalent stress comparison in wear between wheel profiles I–IV and rail profile II rail under condition 2. The equivalent stress of wheel profile I/rail profile II is 609.9 MPa, and the distribution of contact area is similar to that of wheel and rail profiles II, III, and IV. The equivalent stresses of rail profiles II, III, IV increases by 40.4%, 62.3%, and 39.5%, respectively, compared with wheel profile I/rail profile II.

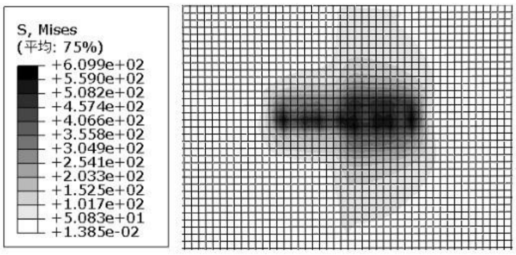

(a) Profile I wheels match profile II rails

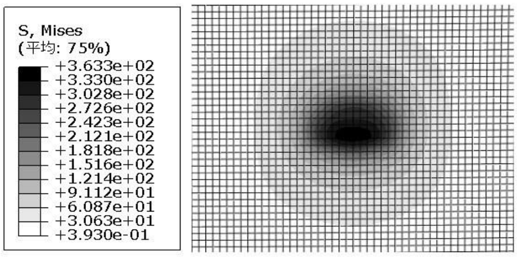

(b) Profile II wheels match profile II rails

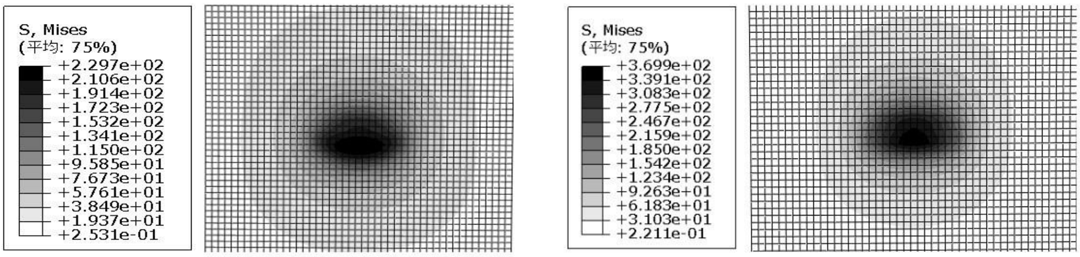

(c) Profile III wheels match profile II rails (d) Profile IV wheels match profile II rails

Fig. 8 Comparison of equivalent stress between wear wheel and rail

5 Conclusion

(1) Under axle load, the matching performance of wheel I/rail II is improved, its contact area is the largest, and its equivalent stress and contact force are minimal.

(2) Under traction force, the matching performance of wheel I/rail II is improved, and the shear stress and equivalent stress are minimal, and thus is ideal.

References

[1] Yang Chunlei, Li Fu, Huang Yunhua. Influence of a vertical suspension on the dynamic behavior of heavy - duty truck wheel and rail [J]. Journal of Southwest Jiaotong University, 2010,46 (5): 820-825.

[2] ZHANG Jian, WEN Ze-feng, SUN Li-ping et al. Design of wheel profile based on rail profile expansion method [J]. Chinese Journal of Mechanical Engineering, 2008,44 (3): 44-49.

[3] SHEVTSOV I Y. Wheel / rail interface optimisation [D]; TU University of Technology, 2008.

[4] Fan Tiehua, Ma Jingbo, Luo Qing Shi and so on. Analysis and prevention of abnormal side grinding of small radius curve [J]. Journal of the China Railway Society, 1990,12 (3): 39-46.

[5] Wang Kaiwen. Calculation of Wheel Contact Point Trace and Wheel / Rail Contact Geometric Parameters [J]. Journal of Southwest Jiaotong University, 1984,18 (1): 89-99.

[6] Jin Xuesong, Liu Qiyue. Wheel - rail tribology [M]. Beijing: China Railway Publishing House, 2004.

[7] Zhang Jian, Song Huiling, Wang Shengwu, and so on. Subway vehicle wheel - rail profile matching analysis [J]. Journal of Dalian Jiaotong University, 2012,33 (5): 1-6